

# Critical finite-size scaling with constraints: Fisher renormalization revisited

Michael Krech

Institut für Theoretische Physik, RWTH Aachen, 52056 Aachen, Germany

**Abstract.** The influence of a thermodynamic constraint on the critical finite-size scaling behavior of three-dimensional Ising and XY models is analyzed by Monte-Carlo simulations. Within the Ising universality class constraints lead to Fisher renormalized critical exponents, which modify the asymptotic form of the scaling arguments of the universal finite-size scaling functions. Within the XY universality class constraints lead to very slowly decaying corrections inside the scaling arguments, which are governed by the specific heat exponent  $\alpha$ . If the modification of the scaling arguments is properly taken into account in the scaling analysis of the data, finite-size scaling functions are obtained, which are *independent* of the constraint as anticipated by analytic theory.

## 1 Introduction

The theoretical investigation of classical spin systems has played a key role in the understanding of phase transitions, critical behavior, scaling, and universality [1,2]. In particular, the classical Ising, the XY, and the Heisenberg model are the most relevant spin models in three dimensions. Each of these simple models represents a universality class which, apart from the spatial dimensionality and the range of the interactions, is characterized by the number of components of the order parameter, e.g., the magnetization in the case of ferromagnetic models. Real systems, however, suffer from various kinds of imperfections, e.g., lattice defects, impurities, or vacancies. In an experiment, which is designed to probe critical behavior as a function of temperature, the presence of, say, impurities on the lattice constitutes a thermodynamic constraint, because in a given sample the impurity concentration will remain constant during the temperature scans. According to the concepts of thermodynamics the impurity concentration  $n_i$  can be written as the derivative of the grand canonical potential with respect to the chemical potential  $\mu_i$  of the impurities, where other parameters like the temperature and the volume of the system are kept fixed. Now the question arises how the critical singularities in the grand canonical potential are affected when the thermodynamic ensemble is changed from 'fixed  $\mu_i$ ' to 'fixed  $n_i$ ', where the location of the critical temperature  $T_c$  depends on the particular values of  $\mu_i$  or  $n_i$ , respectively. The answer to this question has been given a long time ago by Michael Fisher [3]. Provided, that the critical singularities have their usual form in the 'fixed  $\mu_i$ ' ensemble, then the constraint  $n_i = \text{const.}$  amounts to a reparameterization of the reduced temperature  $t = (T - T_c(n_i))/T_c(n_i)$  of the *constrained*

system in terms of the reduced temperature  $\tau = (T - T_c(\mu_i))/T_c(\mu_i)$  of the *unconstrained* system according to [3]

$$t = a\tau + b\tau|\tau|^{-\alpha} + \dots, \quad (1)$$

where  $a$  and  $b$  are nonuniversal constants and the dots indicate higher order contributions. Apart from a linear term (1) contains a singular contribution which is characterized by the critical exponent  $1 - \alpha$  of the entropy density. Which of the two terms in (1) is the leading one for  $t, \tau \rightarrow 0$  depends on the sign of  $\alpha$ . Within the Ising universality class in  $d = 3$  dimensions  $\alpha \simeq 0.109$  [4] so that  $|\tau| \sim |t|^{1/(1-\alpha)}$  to leading order and therefore the critical exponents  $\beta$  (order parameter),  $\gamma$  (susceptibility), and  $\nu$  (correlation length) of the unconstrained system undergo 'Fisher renormalization' in the constrained system according to [3]

$$\beta \rightarrow \beta' = \beta/(1 - \alpha), \quad \gamma \rightarrow \gamma' = \gamma/(1 - \alpha), \quad \nu \rightarrow \nu' = \nu/(1 - \alpha). \quad (2)$$

The specific heat exponent  $\alpha$  requires a more careful analysis, because the specific heat is the temperature derivative of the entropy which in addition to the 'renormalization' displayed in (2) causes a sign change

$$\alpha \rightarrow \alpha' = -\alpha/(1 - \alpha). \quad (3)$$

Note that analytic background contributions to the entropy of the unconstrained system become *singular* in the constrained system due to the singularity in the reparameterization given by (1).

Within the XY universality class in  $d = 3$  the exponent  $\alpha$  is negative [4], where probably the best current estimate  $\alpha \simeq -0.013$  is obtained from an experiment on  ${}^4\text{He}$  near the superfluid transition [5]. For negative  $\alpha$  the linear term on the r.h.s. of (1) is the dominating one for  $\tau \rightarrow 0$ . However, the XY universality class  $\alpha$  is so small, that in practice the singular term in (1) can never be neglected. Instead, the singular contribution to (1) gives rise to very slowly decaying correction terms which must not be confused with Wegner corrections to scaling. These correction terms have to be considered in any scaling analysis in order to obtain correct values for the critical exponents.

If the system is finite, which is necessarily the case for any Monte - Carlo simulation, all critical singularities are rounded, i.e., all quantities are analytic functions of the thermodynamic parameters [6] so that a thermal singularity as shown in (1) does not occur. Critical finite-size rounding effects in, e.g., a cubic box  $L^d$  are captured by *universal* finite-size scaling functions [6,7] which restore all critical singularities in the limit  $L \rightarrow \infty$ . Following the line of argument in [3], (1) then has to be replaced by

$$t = a\tau + \tau|\tau|^{-\alpha}f(\tau L^{1/\nu}), \quad (4)$$

where  $f(x)$  is the finite-size scaling function of the entropy density and  $x = \tau L^{1/\nu}$  is a convenient choice of its scaling argument. For  $\tau \rightarrow 0$  at finite  $L$  the singular prefactor of  $f(x)$  in (4) must be cancelled so that one has

$f(x) = A|x|^\alpha + \dots$  in the limit  $x \rightarrow 0$ , where  $A$  is a nonuniversal constant such that  $f(x)/A$  is a *universal* function of its argument. To leading order in  $\tau$  the reparameterization of the reduced temperature  $t$  of the constrained system is therefore *linear* in the reduced temperature  $\tau$  of the unconstrained system and one finds

$$t = \tau(a + AL^{\alpha/\nu}). \quad (5)$$

According to (5) the finite-size scaling argument  $x$  in the constrained system is given by

$$x = \tau L^{1/\nu} = t L^{1/\nu} / (a + AL^{\alpha/\nu}), \quad (6)$$

where the *shape* of the finite-size scaling functions is maintained [8], i.e., the presence of the constraint *only* affects the form of the scaling argument  $x$ . For  $\alpha > 0$  (6) asymptotically reduces to  $x = t L^{1/\nu'}/A$  for large  $L$  in accordance with Fisher renormalization (see (2)). For  $\alpha < 0$  (6) captures the aforementioned slowly decaying corrections to the asymptotic critical behavior in the XY universality class when a thermodynamic constraint is present. Note that  $A > 0$  for the Ising universality class and that  $A < 0$  for the XY universality class.

In the remainder of this paper a simple spin model is introduced which can be efficiently simulated with existing Monte - Carlo algorithms both with and without constraints in three dimensions. For the Ising and the XY version of the model finite-size scaling according to (6) is tested for the modulus of the order parameter, the susceptibility, and the specific heat.

## 2 Model and simulation method

The model system which is investigated here can be described as an  $O(N - 1)$  symmetric classical 'planar' ferromagnet in a transverse magnetic field. The model Hamiltonian reads

$$\mathcal{H} = -J \sum_{\langle ij \rangle} \sum_{x=1}^{N-1} S_i^x S_j^x - h \sum_i S_i^N, \quad (7)$$

where  $\langle ij \rangle$  denotes a nearest neighbor pair of spins on a simple cubic lattice in  $d = 3$  dimensions. The lattice contains  $L$  lattice sites in each direction and in order to avoid surface effects periodic boundary conditions are applied. Each spin  $\mathbf{S}_i$  is a classical spin with  $N$  components  $\mathbf{S}_i = (S_i^1, S_i^2, \dots, S_i^N)$  with the normalization  $|\mathbf{S}_i| = 1$  for each lattice site  $i$ . The magnetic field  $h$  in (7) only acts on the  $N$ -components of the spins which are not coupled by the exchange interaction  $J$ . From the symmetry of the Hamiltonian it is obvious, that the model belongs to the  $O(N - 1)$  universality class in  $d = 3$ , where nonuniversal quantities like the critical temperature  $T_c = T_c(h)$  depend on the strength of the transverse field  $h$ . Note that  $T_c(h)$  is symmetric around  $h = 0$

and decreases with increasing  $h$ , because the spins become more and more aligned with the  $N$ -direction as  $\pm h$  is increased and due to the normalization condition the typical interaction energy between pairs of spins is decreased.

The Hamiltonian given by (7) defines the unconstrained model. The constraint is imposed on the transverse magnetization  $M$  in the form

$$M \equiv \sum_i S_i^N = \text{const.}, \quad (8)$$

where the Hamiltonian of the constrained model is given by

$$\mathcal{H}_M = -J \sum_{\langle ij \rangle} \sum_{x=1}^{N-1} S_i^x S_j^x = \mathcal{H} + hM. \quad (9)$$

The critical temperature of the constrained model is a symmetric and monotonically decreasing function of the prescribed transverse magnetization  $M$ . The transverse field  $h$  here plays the part of the chemical potential  $\mu_i$  of impurities (see Sect. 1) and the transverse magnetization  $M$  accordingly plays the part of the impurity concentration  $n_i$ . It is also possible to implement  $O(N)$  spin models with impurities or vacancies with diffusion in order to mimic the situation discussed in [3]. However, the fact that the Hamiltonians given by (7) and (9) only require a single 'species' with a single coupling constant leads to some simplifications in the algorithms. Note that the symmetric constrained model ( $M = 0$ ) becomes equivalent to the symmetric unconstrained model ( $h = 0$ ) for sufficiently large lattices. In particular, both versions of the symmetric model have the same  $T_c$ .

The Monte-Carlo algorithm is chosen as a hybrid scheme, where each hybrid Monte-Carlo step consists of 10 updates each of which can be one of the following: one Metropolis sweep of the whole lattice, one single cluster Wolff update [9], or one overrelaxation update of the whole lattice [10], where the latter can only be applied for  $N \geq 3$ . The Metropolis algorithm updates the lattice sequentially and works in the standard way for the unconstrained model. For the constrained model the constraint  $M = \text{const.}$  is observed locally by applying a Kawasaki update dynamics for the  $N^{th}$  components of the spins. For each lattice site  $i$  a nearest neighbor site  $j$  is chosen randomly and a random amount of the  $N^{th}$  spin component is proposed for exchange such that  $S_i^N + S_j^N$  remains constant. Then new spin components  $(S_i^1, S_i^2, \dots, S_i^{N-1})$  are proposed and the spin components  $(S_j^1, S_j^2, \dots, S_j^{N-1})$  are adjusted according to the spin normalization condition  $|S_i| = |S_j| = 1$ . The local change  $\Delta E$  of the configurational energy is calculated according to (9). According to detailed balance the proposed update is accepted with probability  $p(\beta \Delta E)$ , where  $\beta = 1/(k_B T)$ . For our simulation we have chosen  $p(x) = 1/(\exp(x) + 1)$ . Note that all updates must be proposed such that the new spin at lattice site  $i$  is taken from the uniform distribution on the unit sphere in  $N$  dimensions.

The Wolff algorithm also works the standard way [9], except that *only* the first  $N - 1$  components of the spins are used for the cluster growth, i.e., (7) and (9) are treated as planar ferromagnets. This means that a cluster update never changes the  $N^{th}$  component of any spin so that the Wolff algorithm is nonergodic in this case. The cluster update is still a valid Monte-Carlo step in the sense that it fulfills detailed balance, however, in order to provide a valid Monte-Carlo algorithm it has to be used together with the Metropolis algorithm described above in a hybrid fashion. The use of Wolff updates allows us to take advantage of improved estimators [11] for magnetic quantities.

The overrelaxation part of the algorithm performs a microcanonical update of the configuration in the following way. The local configurational energy has the functional form of a scalar product of the spins, where according to (7) and (9) only the first  $N - 1$  components are involved. With respect to the sum of its nearest neighbor spins each spin has a transverse component in the  $(S_i^1, S_i^2, \dots, S_i^{N-1})$  plane which does not enter the scalar product. The overrelaxation algorithm scans the lattice sequentially, determines this transverse component for each lattice site and flips its sign. This overrelaxation algorithm is similar to the one used in [10] and it quite efficiently decorrelates subsequent configurations over a wider range of temperatures around the critical point than the Wolff algorithm. However, overrelaxation can only be applied for  $N \geq 3$ . In the following only the cases  $N = 2$  (transverse Ising) and  $N = 3$  (transverse XY) are considered.

In a typical hybrid Monte-Carlo step we use three Metropolis ( $M$ ), seven single cluster Wolff ( $C$ ) updates for  $N = 2$  and three Metropolis, five single cluster Wolff, and two overrelaxation updates ( $O$ ) for  $N = 3$  in the critical region of the models. The individual updates are mixed automatically in the program so that the update sequences  $(M\ C\ C\ M\ C\ C\ M\ C\ C\ C)$  for  $N = 2$  and  $(M\ C\ C\ M\ O\ C\ M\ C\ C\ O)$  for  $N = 3$  are generated as one hybrid Monte-Carlo step. The shift register generator R1279 given by the recursion relation  $X_n = X_{n-p} \oplus X_{n-q}$  for  $(p, q) = (1279, 1063)$  is used as the random number generator. Generators like this are known to cause systematic errors in combination with the Wolff algorithm [12]. However, for lags  $(p, q)$  as large as the ones used here these errors will be far smaller than typical statistical errors. They are further reduced by the hybrid nature of our algorithm due to the presence of several Metropolis updates in one hybrid Monte-Carlo step [13].

The hybrid Monte-Carlo scheme described above is employed for lattice sizes  $L$  between  $L = 20$  and  $L = 80$ . For each system size and temperature we perform at least 10 blocks of  $10^3$  hybrid steps for equilibration followed by  $10^4$  hybrid steps for measurements. Each measurement block yields an estimate for all static quantities of interest and from these we obtain our final estimates and estimates of their statistical error following standard procedures. At the critical point (see below) two or three times as many updates have been performed. The integrated autocorrelation time of the hybrid algorithm is

determined by the autocorrelation function of the energy or, equivalently, the modulus of the order parameter, which yield the slowest modes for the Wolff algorithm. The autocorrelation times are generally rather short, at the critical point they range from about 5 hybrid Monte-Carlo steps for  $L = 20$  to about 10 hybrid Monte-Carlo steps for  $L = 80$ . The values for the equilibration and measurement periods given above thus translate to roughly 100 and 1000 autocorrelation times, respectively. In order to obtain the best statistics for magnetic quantities a measurement is made after every hybrid Monte-Carlo step. All error bars quoted in the following correspond to one standard deviation. The simulations have been performed on the DEC alpha AXP workstation cluster at the Physics Department and on HP RISC8000 workstations at the Computer Center of the RWTH Aachen.

### 3 Ising universality class

For  $N = 2$  (7) and (9) describe a classical Ising model in a (fixed) transverse field or with fixed transverse magnetization, respectively. In the following we will only consider the constrained model with the symmetric constraint  $M = 0$  and with the constraint  $m \equiv M/L^3 = 1/\sqrt{2}$ . The symmetrically constrained model does not show Fisher renormalization [3] and we therefore use this case for tests of the algorithm and for the production of data representative of the Ising universality class in  $d = 3$ . The constraint  $m = \text{const.} \neq 0$  breaks the  $S_i^N \rightarrow -S_i^N$  symmetry of the model and Fisher renormalization should become visible within a certain temperature window around  $T_c = T_c(m)$ . The width of this window is of course a nonuniversal property of the model and in particular one expects this window to widen as  $m$  is increased. Due to the spin normalization condition  $m$  cannot exceed unity and one therefore also expects, that critical behavior becomes very difficult to resolve numerically if  $m$  is too close to its maximum value. Therefore,  $m = 1/\sqrt{2}$  is chosen as a compromise between good resolution in the critical regime and a prominent Fisher renormalization effect.

The critical temperatures  $T_c(m = 0)$  and  $T_c(m = 1/\sqrt{2})$  are determined from temperature scans of the Binder cumulant ratio according to standard procedures [14]. We obtain the following reduced critical coupling constants  $K_c(m) \equiv J/k_B T_c(m)$ :

$$K_c(0) = 0.41638 \pm 0.00005 \quad \text{and} \quad K_c(1/\sqrt{2}) = 0.6371 \pm 0.0001. \quad (10)$$

The corresponding estimates for the Binder cumulant ratio obtained for  $m = 0$  and  $m = 1/\sqrt{2}$  agree with previous estimates obtained for the Ising universality class within two standard deviations [15], where for the latter choice of  $m$  Wegner corrections to scaling are considerable and must be subtracted in order to obtain a reliable estimate. In order to obtain an estimate

for the exponent  $\nu$  which enters the finite-size scaling argument according to (6) the cumulant

$$X \equiv \frac{\partial}{\partial T} \ln \langle \phi^2 \rangle = \frac{1}{k_B T^2} \left( \frac{\langle \phi^2 \mathcal{H}_M \rangle}{\langle \phi^2 \rangle} - \langle \mathcal{H}_M \rangle \right) \quad (11)$$

has been measured, where  $\phi = L^{-3} \sum_i S_i^1$  is the order parameter. At the critical temperature  $T_c(m)$  the scaling behavior  $X \sim x/t$  is expected (see (6)). Corresponding numerical results for  $m = 0$  and  $m = 1/\sqrt{2}$  are displayed in Fig.1 on a double logarithmic scale. The data are compatible with simple

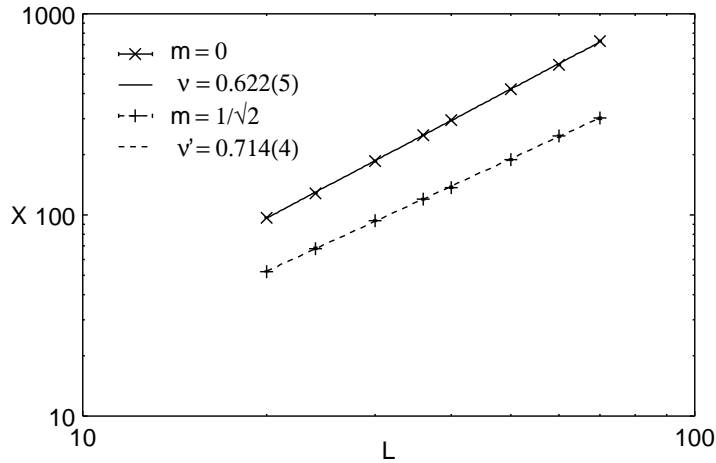


**Fig. 1.** Cumulant  $X$  at the critical point for  $m = 0$  ( $\times$ ) and  $m = 1/\sqrt{2}$  ( $+$ ). The solid and dashed lines display power law fits to the data for  $30 \leq L \leq 70$  for  $m = 0$  and  $m = 1/\sqrt{2}$ , respectively

power laws, where the exponents  $\nu = 0.622 \pm 0.005$  ( $m = 0$ ) and  $\nu' = 0.714 \pm 0.004$  ( $m = 1/\sqrt{2}$ ) have been obtained. Compared to the best currently known estimate  $\nu \simeq 0.630$  [4] the above estimate is too small and only agrees with the theoretical value within two standard deviations. A more thorough analysis shows that the discrepancy can be explained by a mismatch of the order  $5 \times 10^{-5}$  between the actual critical temperature and the estimate used here (see (10)), which on the other hand is of the same magnitude as the statistical error of  $K_c(0)$ . The agreement between the above estimate for  $\nu' = \nu/(1 - \alpha)$  and the theoretical value  $\nu' \simeq 0.708$  [4] is better, however, it may again be affected by a mismatch between the actual value of  $T_c(1/\sqrt{2})$  and the estimate used here. If the literature values for  $\nu$  and  $\alpha$  are substituted in (6), where  $a$  and  $A$  are used as fit parameters,  $a/A \simeq 0.1$  is obtained which is small enough to be ignored in the scaling analysis (see below).

The finite-size scaling analysis has been performed for several thermodynamic quantities, in particular, the average modulus of the order parameter  $\langle|\phi|\rangle$ , the susceptibilities

$$\chi_+ \equiv \frac{L^3}{k_B T} \langle \phi^2 \rangle, \quad \chi_- \equiv \frac{L^3}{k_B T} (\langle \phi^2 \rangle - \langle |\phi| \rangle^2), \quad (12)$$

and the specific heat  $C$ . Data will only be shown for  $\langle|\phi|\rangle$ ,  $\chi_-$ , and  $C$ , because the finite-size scaling functions for  $\langle|\phi|\rangle$  and  $\chi_+$  are very similar. According to finite-size scaling theory it must be possible to collapse the data for all  $m$  onto one and the same curve, where two nonuniversal scaling factors are required for each quantity. One scaling factor adjusts the magnitude of the scaling argument  $x$  (see (6)), the other adjusts the absolute normalization of the quantity. Note that the former scaling factor must be the same for *all* quantities. For  $m = 0$  the scaling argument  $x = tL^{1/\nu}$  is used, whereas for  $m = 1/\sqrt{2}$  the choice  $x = tL^{(1-\alpha)/\nu}/A$  has been made, where  $A \simeq 1.1$  and the coefficient  $a$  in (6) has been neglected. The exponents  $\nu$  and  $\alpha$  are taken from the literature [4]. The scaling plot of  $\langle|\phi|\rangle$  is shown in Fig.2, where the

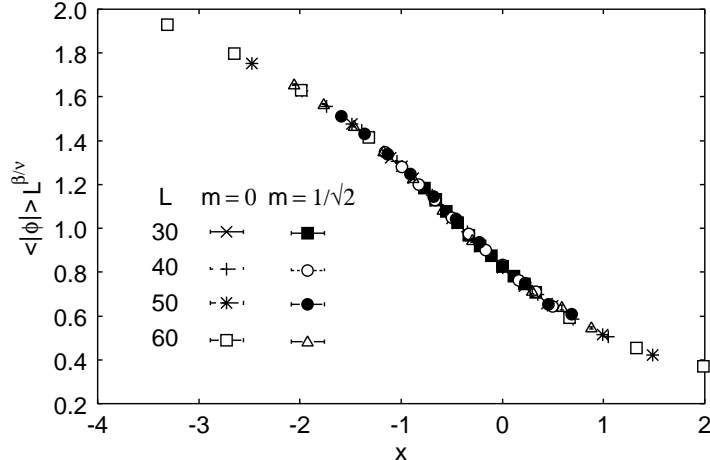


**Fig. 2.** Scaling plot of  $\langle|\phi|\rangle$  for  $L = 30, 40, 50$ , and  $60$  for  $m = 0$  and  $m = 1/\sqrt{2}$ . The reduced temperature  $t$  has been varied between  $-0.007$  and  $0.003$ . Statistical errors are much smaller than the symbol sizes

absolute normalization of the data for  $m = 1/\sqrt{2}$  can be adjusted to the  $m = 0$  data by a scale factor of  $\sim 0.7$  as one would expect from simple mean field arguments. As shown in Fig.2, the expected data collapse can be reproduced rather well, where the literature value for the exponent  $\beta/\nu = 0.5168$  [4] has been used. The same holds for the susceptibility  $\chi_-$  which is displayed in Fig.3, where  $\gamma/\nu = 2 - \eta = 1.967$  is also taken from [4]. The absolute

magnitudes of  $\chi_-/L^{\gamma/\nu}$  for  $m = 0$  and  $m = 1/\sqrt{2}$  are different by a factor of about 0.5 which is in accordance with simple mean field arguments. Note that the scaling function of  $\chi_-$  has a maximum for  $x < 0$  [16].

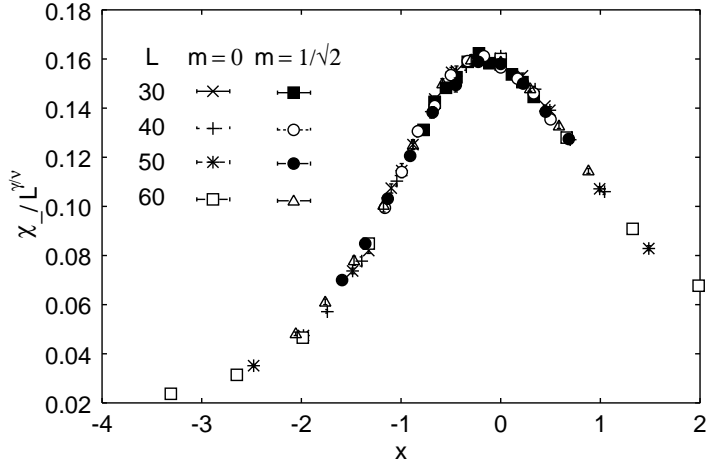


**Fig. 3.** Scaling plot of  $\chi_-$  for  $L = 30, 40, 50$ , and  $60$  for  $m = 0$  and  $m = 1/\sqrt{2}$ . The reduced temperature  $t$  has been varied between  $-0.007$  and  $0.003$ . Statistical errors are much smaller than the symbol sizes

The specific heat  $C$  requires a somewhat different treatment due to the fact that unlike the other quantities presented so far the specific heat requires an *additive* renormalization within renormalized field theory [16]. For the data analysis this means that scaling can only be obtained after a suitable subtraction is applied to the specific heat. One option to obtain scaling is to subtract the bulk specific heat  $C_b^0(t)$  at a reference reduced temperature  $t = t_0$  which are given by

$$C_b^0(t) = \frac{A_{\pm}}{\alpha} |t|^{-\alpha} + B \quad \text{and} \quad t_0 = (L/\xi_{\pm}^0)^{-1/\nu}, \quad (13)$$

where  $A_{\pm}$  and  $B$  are nonuniversal constants and  $\xi_{\pm}^0$  is the amplitude of the correlation length. The index  $\pm$  refers to temperatures above or below  $T_c(m)$ , respectively. The reference reduced temperature chosen in (13) is positive and therefore only  $A_+$  and  $\xi_+^0$  are needed. Specifically, the choice  $\nu = 0.630$ ,  $\alpha = 0.109$  [4],  $A_+ = 0.1552$ ,  $B = -1.697$ , and  $\xi_+^0 = 0.495$  [16] guarantee scaling of the *relative* specific heat  $\Delta C^0 \equiv C - C_b^0(t_0)$  for the Ising model in  $d = 3$ . Note that  $\xi_+^0$  is measured in units of the lattice constant. For the data to be analyzed here the subtraction defined by (13) is only valid for the case  $m = 0$ , where  $\Delta C^0$  scales as  $L^{\alpha/\nu}$ . For  $m = 1/\sqrt{2}$  Fisher renormalization

according to (1) must be applied to  $C_b^0(t)$  in order to obtain the correct form  $C_b^m(t)$  of the subtraction. The result is

$$C_b^m(t) = \frac{A'_+}{\alpha} |t|^{\alpha/(1-\alpha)} + B' \quad \text{and} \quad t_0 = (L/\xi_+^0)^{(\alpha-1)/\nu}, \quad (14)$$

where  $A'_+ = -0.1728$ ,  $B' = 1.598$ , and  $\xi_+^0 = 0.495$  is not changed. The scaling factor  $L^{\alpha/\nu}$ , which usually governs the finite-size scaling of the specific heat, is cancelled here, i.e., one expects data collapse for  $\Delta C^0/L^{\alpha/\nu}$  and  $\Delta C^m \equiv C - C_b^m(t_0)$  up to an overall scale factor of about 0.5. The result of the data analysis is shown in Fig.4. The data collapse reasonably well onto

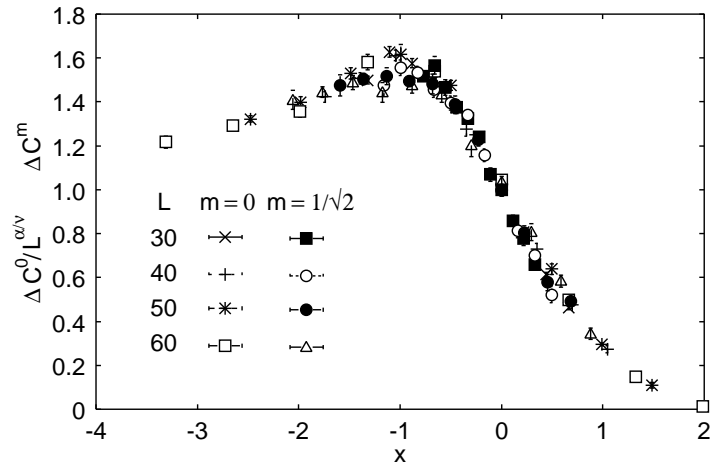


**Fig. 4.** Relative specific heats  $\Delta C^0/L^{\alpha/\nu}$  for  $m = 0$  and  $\Delta C^m$  for  $m = 1/\sqrt{2}$  for  $L = 30, 40, 50$ , and  $60$ . The reduced temperature  $t$  has been varied between  $-0.007$  and  $0.003$

a single curve except near the maximum of the scaling function, where also the scatter of the individual data is substantial due to a few bad samples for  $L = 50$  and  $60$ . However, there are also systematic deviations from scaling in the data, because the maximum in the scaling functions for the  $m = 0$  data is more pronounced than in the  $m = 1/\sqrt{2}$  data. These deviations could be due to enhanced Wegner corrections to scaling for  $m = 1/\sqrt{2}$  as compared to  $m = 0$ .

#### 4 XY universality class

For  $N = 3$  (7) and (9) describe a classical XY model in a (fixed) transverse field or with fixed transverse magnetization, respectively. As for the case

$N = 2$  we will only consider the constrained model with the symmetric constraint  $m = 0$  and with the constraint  $m = 1/\sqrt{2}$  in the following. The symmetrically constrained model is again used for algorithmic tests and data production for the XY universality class. The nonsymmetric constrained XY model does not show Fisher renormalization, however, according to (6) very slowly decaying corrections to the asymptotic critical behavior are expected, which will be discussed in the following. First, the cumulant  $X$  defined by (11) is evaluated at the critical point, which is given by the reduced coupling constants

$$K_c(0) = 0.6444 \pm 0.0001 \quad \text{and} \quad K_c(1/\sqrt{2}) = 1.1126 \pm 0.0003, \quad (15)$$

respectively. The result for  $X$  is displayed in Fig.5. For  $m = 0$  the data can

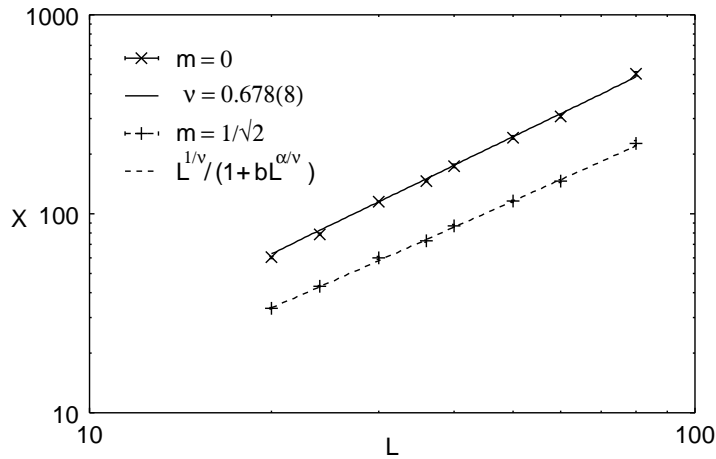


**Fig. 5.** Cumulant  $X$  at the critical point for  $m = 0$  (x) and  $m = 1/\sqrt{2}$  (+). The solid and dashed lines display fits to the data for  $30 \leq L \leq 80$  for  $m = 0$  and  $m = 1/\sqrt{2}$ , respectively (see main text)

be fitted by a power law  $\sim L^{1/\nu}$ , where  $\nu = 0.678 \pm 0.008$  is obtained which agrees with the best current estimate  $\nu = 0.671$  [4]. For  $m = 1/\sqrt{2}$  the data can also be fitted by a power law, however, the resulting exponent  $\nu$  only has the meaning of an effective exponent which does not fit into the XY universality class. As shown in Fig.5 the expression  $x/t$  according to (6) also yields a very good representation of the data where the parameter  $b$  in Fig.5 is given by  $b = A/a = -0.941$ . The exponents used in the fit (XY universality class) are taken from [4]. The value of the Binder cumulant found here agrees with results reported in the literature for the standard (plane rotator) XY model [17], however, Wegner corrections to scaling become quite substantial for  $m = 1/\sqrt{2}$ .

In the following scaling analysis the finite-size scaling argument for the case  $m = 0$  takes its standard form  $x = tL^{1/\nu}$  and for  $m = 1/\sqrt{2}$  the combination  $x = tL^{1/\nu}/(1 + bL^{\alpha/\nu})$  for  $b = -0.941$  takes care of the slowly decaying correction terms to the asymptotic critical behavior caused by the very small and negative value of  $\alpha$  in the XY universality class. As in Sect. 3 we consider  $\langle|\phi|\rangle$ ,  $\chi_+$ ,  $\chi_-$ , and the specific heat  $C$  in the scaling analysis. The scaling functions for  $\langle|\phi|\rangle$  and  $\chi_+$  again look very similar so that we do not reproduce scaling plots for  $\chi_+$  here. The result for  $\langle|\phi|\rangle$  is shown in Fig.6, where the order parameter  $\phi \equiv L^{-3} \sum_i (S_i^1, S_i^2)$  has two components here. The data collapse very well onto a single curve. Note that the absolute

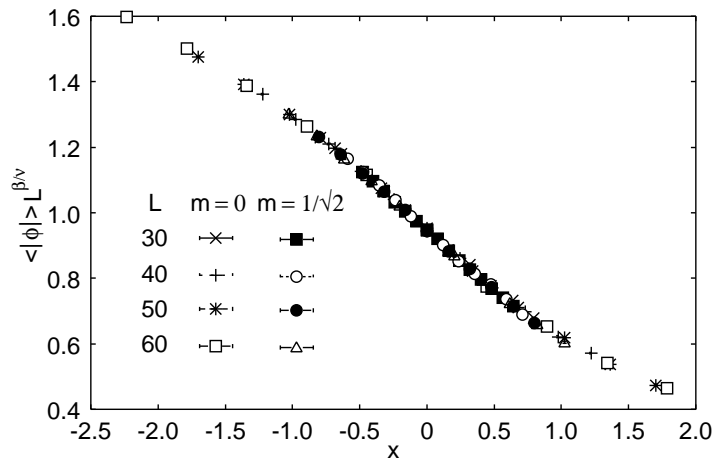


**Fig. 6.** Scaling plot of  $\langle|\phi|\rangle$  for  $L = 30, 40, 50$ , and  $60$  for  $m = 0$  and  $m = 1/\sqrt{2}$ . The reduced temperature  $t$  has been varied between  $-0.005$  and  $0.005$ . Statistical errors are much smaller than the symbol sizes

magnitudes of  $\langle|\phi|\rangle$  for  $m = 0$  and  $m = 1/\sqrt{2}$  are again related by a factor of  $\sim 0.7$  as suggested by mean-field arguments. The values for the critical exponents  $\nu = 0.671$  and  $\beta = 0.347$  are taken from the literature [4]. The susceptibility  $\chi_-$  can be treated essentially as described in Sect.3, where the exponent  $\gamma/\nu = 2 - \eta = 1.965$  is taken from [4]. The result of the scaling analysis is displayed in Fig.7. The data do not collapse as well as in Fig.3. Especially near the maximum of the scaling function the scatter of the data is substantially larger than in Fig.3. Slight systematic deviations from scaling for  $m = 1/\sqrt{2}$  are observed which may again be due to enhanced Wegner corrections to scaling as compared to  $m = 0$ . Note that contrary to Fig.3 the scaling function of  $\chi_-$  has a maximum for  $x > 0$  in the XY universality class.

The specific heat  $C$  of the XY model also requires a subtraction before scaling is obtained [18]. The subtraction  $C_b^0(t_0)$  is again used in the form

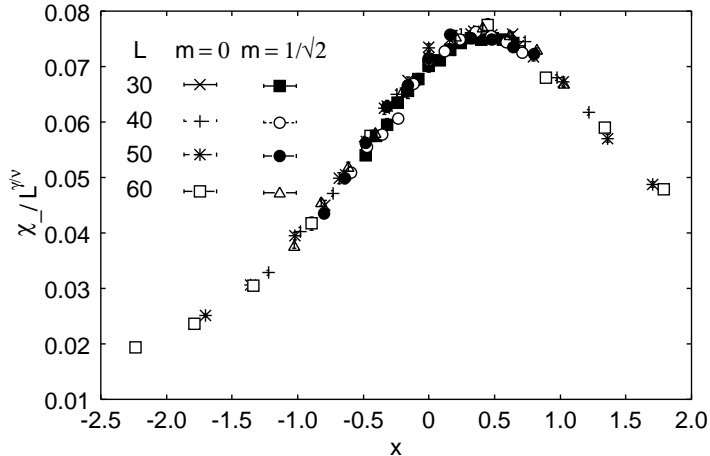


**Fig. 7.** Scaling plot of  $\chi_-$  for  $L = 30, 40, 50$ , and  $60$  for  $m = 0$  and  $m = 1/\sqrt{2}$ . The reduced temperature  $t$  has been varied between  $-0.005$  and  $0.005$ . Statistical errors are much smaller than the symbol sizes

given by (13), where  $A_+ = 0.42$ ,  $\alpha = -0.013$ ,  $B = -A_+/\alpha$ , and  $\xi_+^0 = 1.0$  are used here which differ somewhat from the choices made for the standard XY model in [18]. It turns out, that the quality of the data collapse for the relative specific heat  $\Delta C^0 = C - C_b^0(t_0)$  for  $m = 0$  is rather insensitive to the choice of  $\xi_+^0$ . The form of the subtraction  $C_b^m(t_0)$  for  $m = 1/\sqrt{2}$  requires a little analysis in order to include the slowly varying corrections to the asymptotic behavior coming from (1). One obtains the approximate form

$$C_b^m(t_0) = \frac{A_+/\alpha}{1 + ct_0^{-\alpha}} \left[ \left( \frac{t_0}{1 + ct_0^{-\alpha}} \right)^{-\alpha} - 1 \right], \quad t_0 = L^{-1/\nu}(1 + bL^{\alpha/\nu}), \quad (16)$$

where  $b = -0.941$  (see Fig.5),  $A_+ = 0.42$  as before, and  $c \simeq 2.0$  for optimal data collapse. The resulting scaling plot of  $\Delta C^0$  and  $\Delta C^m \equiv C - C_b^m(t_0)$  is displayed in Fig.8. The overall shape of the scaling function is similar to the one shown in Fig.4. However, the scatter of the data near the maximum is so strong, that data collapse cannot be obtained in this region. In part this deficiency in the data may be due to the presence of 'bad' samples, e.g, for  $L = 50$  and  $m = 0$  at  $t = -0.003$  and  $t = -0.002$  and for  $L = 60$  and  $m = 1/\sqrt{2}$  at  $t = -0.005$  and  $t = -0.003$ . Apart from that deviations from scaling as in Fig.4 may be present which are due to an enhancement of Wegner corrections to scaling for  $m = 1/\sqrt{2}$  as compared to the case  $m = 0$ . However, Figs.6 - 8 confirm, that the choice of the scaling variable  $x$  given by (6) captures the slowly decaying correction term inside the scaling argument in an appropriate way and that furthermore the finite-size scaling behavior of

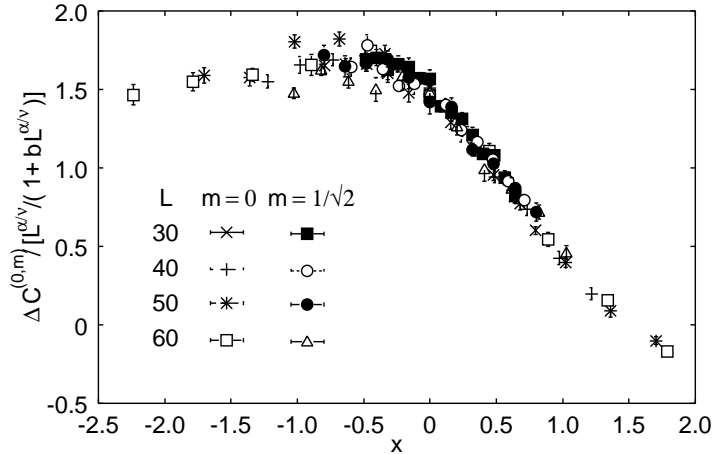


**Fig. 8.** Relative specific heats  $\Delta C^{(0,m)} / [L^{\alpha/\nu} / (1 + bL^{\alpha/\nu})]$  with  $b = 0$  for  $m = 0$  and  $b = -0.941$  for  $m = 1/\sqrt{2}$  for  $L = 30, 40, 50$ , and  $60$ . The reduced temperature  $t$  has been varied between  $-0.005$  and  $0.005$

constrained models in the Ising and the XY universality class can be treated on the same footing.

## 5 Summary and conclusions

The influence of constraints on the critical finite-size scaling behavior of Ising and XY models has been investigated by Monte-Carlo simulations of  $O(N-1)$  planar ferromagnets with fixed transverse magnetization. The theoretical idea that only the form of the scaling argument is modified, whereas the shape of the universal scaling functions remains unchanged is verified within the statistical uncertainty of the data for the modulus of the order parameter, the susceptibilities  $\chi_+$  (not shown) and  $\chi_-$ , and the specific heat. The form of the scaling argument used here allows to deal with critical finite-size effects in constrained Ising and XY models on the same footing, where constrained Heisenberg models can be included as well. Within the Ising universality class the finite-size behavior is consistent with the Fisher renormalization of critical exponents. In the XY universality class slowly decaying corrections to the asymptotic critical behavior are generated which are captured systematically by the analytic form of the scaling argument. The treatment of these corrections within the XY universality class may serve as a paradigm for the finite-size scaling analysis of dynamic quantities, where the constraints imposed here reappear as conserved quantities which are statically or dynamically coupled to the order parameter. These corrections may also be important for the interpretation of spin dynamics data for planar ferromag-

nets, where the energy of the system is conserved during the simulated time evolution of spin models similar to the ones investigated here.

### Acknowledgments

The author gratefully acknowledges many helpful discussions with V. Dohm and financial support of this work through the Heisenberg program of the Deutsche Forschungsgemeinschaft.

### References

1. Amit D. J. (1978) *Field Theory, the Renormalization Group, and Critical Phenomena*, McGraw-Hill, New York
2. Parisi G. (1988) *Statistical Field Theory*, Addison-Wesley, Wokingham
3. Fisher M. E. (1968) *Phys. Rev.* **176**, 257
4. Le Guillou J. C., Zinn-Justin J. (1985) *J. Phys. (France) Lett.* **46**, L137; Guida R., Zinn-Justin J. (1998) *J. Phys. A* **31**, 8103
5. Lipa J. A., Swanson D. R., Nissen J. A., Chui T. C. P., Israelsson U. E. (1996) *Phys. Rev. Lett.* **76**, 944
6. Fisher M. E. (1971) in: Green M. S. (Ed.) *Proceedings of the 1970 Enrico Fermi School of Physics, Varenna, Italy*, Course No. LI Academic, New, York, p.1; Fisher M. E., Barber M. N. (1972) *Phys. Rev. Lett.* **28**, 1516
7. Barber M. N. (1983) in: Domb C., Lebowitz J. L. (Eds.) *Phase Transitions and Critical Phenomena*, Vol. 8, Academic, New York, p. 145; Privman V. (1990) in: Privman V. (Ed.) *Finite Size Scaling and Numerical Simulation of Statistical Systems*, World Scientific, Singapore
8. Dohm V. (1998) private communication
9. Wolff U. (1989) *Phys. Rev. Lett.* **62**, 361
10. Chen K., Landau D. P. (1994) *Phys. Rev. B* **49**, 3266
11. Hasenbusch M. (1990) *Nucl. Phys. B* **333**, 581
12. Ferrenberg A. M., Landau D. P., Wong Y. J. (1992) *Phys. Rev. Lett.* **69**, 3382; Shchur L. N., Blöthe H. W. J. (1997) *Phys. Rev. E* **55**, R4905
13. Ferrenberg A. M., Landau D. P. unpublished
14. Chen K., Ferrenberg A. M., Landau D. P. (1993) *Phys. Rev. B* **48**, 3249
15. Blöthe H. W., Luijten E., Heringa J. R. (1995) *J. Phys. A* **28**, 6289
16. Esser A., Dohm V., Chen X. S. (1995) *Physica A* **222**, 355; Chen X. S., Dohm V., Talapov A. L. (1996) *Physica A* **232**, 375
17. Gottlob A. P., Hasenbusch M. (1993) *Physica A* **201**, 593
18. Chen X. S., Dohm V., Esser, A. (1995) *J. Phys. I France* **5**, 205; Schultka N., Manousakis E. (1995) *Phys. Rev. B* **52**, 7528